Relative rotation rates as the abelianization of the pure braid group

N. B. Tufillaro*
Aqualytics, P. O. Box 1028, Corvallis, Oregon 97333, USA
(Dated: August 20, 2026)

We show that the relative rotation rates of Solari and Gilmore are the image of the periodic-orbit braid under the abelianization of the pure braid group, $P_n \to \mathbb{Z}^{n(n-1)/2}$. The Nielsen–Thurston data lie in the kernel $[P_n, P_n]$, so no function of the rates recovers them. This accounts for the failure of the self-rotation-rate spectrum to fix horseshoe braid type beyond period 10, a failure we exhibit in six tabulated period-11 orbits. The relation clarifies the different uses of exponent sums and linking numbers to identify chaotic systems.

Solari and Gilmore introduced the relative rotation rate (RRR) to describe how pairs of periodic orbits wind about one another in a periodically driven flow [1]. Two orbits of periods p_A and p_B close up together after $p_A p_B$ drive periods, and the vector from one to the other turns through a whole number of revolutions. The relative rotation rate $R_{ij}(A, B)$ is the average number of turns per period. The table of these ratios over all orbit pairs is the intertwining or RRR matrix. It was proposed first as a fingerprint for strange attractors [2] and then as the basis of a classification of chaos by integers [3, 4]. The proposal worked. Templates were identified for the Duffing oscillator, the Belousov–Zhabotinskii reaction, an NMR laser, a laser with a saturable absorber, and a vibrating string by matching measured linking numbers and rotation rates against cataloged forms [3–9]. The same data track bifurcations and orbit forcing. Two orbits can meet in a saddle–node bifurcation only if their rotation rates against every other orbit agree [1]. Linking numbers of saddle–node pairs generate forcing relations, computed through period 8 for horseshoe-type templates [4, 10].

These invariants also met limits at definite periods. The exponent sum, the total signed crossing count of the orbit braid, distinguishes horseshoe braid types through period 8, but not beyond [11]. The spectrum of self-relative rotation rates does better. Gilmore and Lefranc conjectured that orbits sharing an RRR spectrum share a braid type; they report that this holds for horseshoe orbits through period 10 but fails at period 11 [9, Sects. 4.5.3 and 9.3.3.2]. Mindlin *et al.* observed early that any finite set of periodic orbits of a three-dimensional flow with a Poincaré section is an element of the braid group, up to conjugacy [5]. Their attention then turned to branched manifolds and to invariants easier to compute than the braid itself. This Letter points out that the braid itself is now computationally tractable and its utility is worth revisiting.

The key observation is that the relative rotation rates of a collection of periodic orbits are the image of its braid under the abelianization of the pure braid group. This is the homomorphism $P_n \to P_n^{\mathrm{ab}} \cong \mathbb{Z}^{n(n-1)/2}$ that keeps the pairwise winding of strands and discards the rest. The crossing-count definition given as Eq. (A4) in the Appendix of Ref. [1] is this homomorphism written in coordinates. The kernel is the commutator subgroup $[P_n, P_n]$, and the Nielsen–Thurston data of the braid—its type, its dilatation, its topological entropy [12, 13]—live there. The identification shows where the rotation rates are complete and why the period-11 conjecture fails. Gilmore and Lefranc describe the relation between braid type and entropy as an active area in which many questions remain open [9, Sect. 9.6]; the identification addresses one of them.

Abelianization in relation to braids and chaotic dynamics was recently discussed by Thiffeault, whose monograph on braids for applied dynamics abelianizes the braid's Artin action on the fundamental group of the punctured disc [14]. In that analysis only the permutation survives, and the conclusion drawn there is that "too much is lost in the process of Abelianizing" [14]. That map abelianizes the group the braid *acts on*; ours abelianizes the group of *braids*, and what survives is exactly the intertwining matrix (Table I).

We first recall how the rotation rates are measured. Let f be the return map of a flow on a disc-like cross section Σ. For a system driven at period τ the phase space is $D^2 \times S^1$, the section is the disc at a fixed drive phase, and f is the stroboscopic map [1]. A period-p_A orbit A meets Σ in p_A points $a_1, \ldots, a_{p_A}$, visited cyclically. The canonical example is the suspension of the Smale horseshoe map, whose orbits are tabulated across this literature [1, 9, 11, 15]. Fix orbits A and B, choose starting points (a_i, b_j), and follow the difference vector $\boldsymbol{\delta}_{ij}(t) = \mathbf{x}_A(t) - \mathbf{x}_B(t)$ as the drive runs. After $p_A p_B$ periods both orbits have closed and the argument of $\boldsymbol{\delta}_{ij}$ has advanced by an integer multiple of 2π. The relative rotation rate is the average advance per period,

$$R_{ij}(A, B) = \frac{1}{2\pi\, p_A p_B} \oint d \arg \boldsymbol{\delta}_{ij}, \tag{1}$$

a rational number with denominator dividing $p_A p_B$ [1]. We count a rotation as positive when it is counterclockwise seen looking into the flow, following Ref. [1]; Ref. [16] adopts the opposite sign. Self-rates $R_{ij}(A, A)$ are defined by the same integral for $i \neq j$, with $R_{ii}(A, A) = 0$ by convention. Summing over starting points recovers the linking and self-linking numbers, $\mathrm{Lk}(A, B) = \sum_{i,j} R_{ij}(A, B)$, with no residual factor [1].

* Contact author: nick@aqualytics.eco

The integral is a crossing count. The Appendix of Ref. [1] gives four equivalent definitions of R_{ij}. The last of them, its Eq. (A4), cuts A and B into segments between successive section crossings, projects along the flow, and counts the signed crossings $\sigma_{r,s}$ of segment r of A over segment s of B:

$$R_{ij}(A,B) = \frac{1}{p_A p_B} \sum_{n=1}^{p_A p_B} \sigma_{i+n,\, j+n}. \tag{2}$$

Each full turn of the difference vector is one signed passage of one orbit strand over the other, so the rotation rate and the crossing count record the same events. Because Eq. (2) makes no reference to time, Solari and Gilmore observed that the concept extends to autonomous three-dimensional flows [1]. The extension must supply its own section and its own suspension, subtleties we treat elsewhere. Here the drive fixes both, and the rotation rates are well-defined invariants of the flow.

Now take a finite collection of orbits $\{A^1, \ldots, A^m\}$ with periods $p_1, \ldots, p_m$, meeting Σ in $n = \sum_a p_a$ points, and let the drive run through $N = \mathrm{lcm}(p_1, \ldots, p_m)$ periods. Each orbit point travels along its orbit and returns to itself, so the n points trace n strands in $D^2 \times [0, N\tau]$: a geometric braid β. Since every strand ends where it began, β lies in the pure braid group $P_n \subset B_n$, the subgroup of braids inducing the trivial permutation. The braid type of the collection is the conjugacy class of β in B_n modulo the full twist Δ^2, a quotient that absorbs relabelings, the identification of Σ with a standard disc, and the choice of suspension [13, 17]. The pure braid group abelianizes onto a free abelian group with one coordinate per pair of strands,

$$\mathrm{ab}\colon\ P_n \longrightarrow P_n^{\mathrm{ab}} = P_n/[P_n, P_n] \;\cong\; \mathbb{Z}^{n(n-1)/2}, \tag{3}$$

and the coordinates are linking numbers [18]. The generator A_{kl}, in which strand l makes one loop about strand k, maps to the unit vector e_{kl}. A general β maps to the vector of pairwise strand linking numbers $\mathrm{Lk}_{kl}(\beta)$, each half the signed count of crossings between strands k and l. The winding of the difference vector of strands i and j over the N-period suspension is $2\pi\, \mathrm{Lk}_{ij}(\beta)$. Equation (1) averages over $p_A p_B$ periods, but the difference vector closes after $\mathrm{lcm}(p_A, p_B)$ periods, a span dividing both $p_A p_B$ and N. Each window holds a whole number of these cycles, so the average turn per period is the same over either. Comparing with Eqs. (1) and (2) gives, entry for entry,

$$R_{ij} = \frac{1}{N}\, \mathrm{Lk}_{ij}(\beta). \tag{4}$$

The intertwining matrix of an orbit collection is the abelianization of its pure braid, normalized per period. Self-rates are the intra-orbit strand linkings per period, and summing the coordinates of $\mathrm{ab}(\beta)$ blockwise gives N times the orbit-pair linking numbers. Equation (2) is the homomorphism (3) written in coordinates, and the rotation rates and $\mathrm{ab}(\beta)$ determine each other exactly. Three abelianizations now appear in this literature. Table I separates them; only the last reproduces the rotation rates.

Every homomorphism is blind to its kernel, and here the kernel is the commutator subgroup $[P_n, P_n]$. Two collections whose braids differ by an element of $[P_n, P_n]$ have identical rotation rates, in every entry. The Nielsen–Thurston type of β, its dilatation, and its topological entropy vary within a single abelianization class, so none of them is a function of the intertwining matrix. The height and the depth, the rational braid-type invariants that order the creation of horseshoe orbits [19], are likewise defined through the braid type, not through the abelian data. The published tables of Ref. [11] lay the two kinds of data side by side, listing the exponent sum beside Thurston type, height, depth, and train-track entropy for every horseshoe braid through period 11. That the abelian invariants give out at finite period—8 for the exponent sum, 10 for the intertwining matrix—reflects this one kernel: every distinction they miss lies in $[P_n, P_n]$. The exponent sum is the image of β in $B_n^{\mathrm{ab}} \cong \mathbb{Z}$, the coarsest map in Table I, and separates horseshoe braid types through period 8 [11]. The intertwining matrix is the image in P_n^{ab} and separates them through period 10 [4, 9]. Both are abelianizations, differing only in resolution: the exponent sum records one integer where the intertwining matrix records a winding number for every pair of strands. Each holds until the horseshoe family grows large enough that two orbits of different braid type share the same abelianized image. At period 11, exactly where the conjecture fails [9], Table III of Ref. [11] contains six pseudo-Anosov orbits, $s11^{35}$, $s11^{36}$, $s11^{43}$, $s11^{47}$, $s11^{50}$, and $s11^{54}$, sharing rotation number $4/11$ and exponent sum 32. With the points of each orbit numbered in the order the orbit visits them, R_{ij} depends only on the separation $d = j - i \bmod 11$, and all six share the same values: $R = 4/11$ at $d = 1, 10$ and $R = 3/11$ at $d = 2, \ldots, 9$.[1] Their images in P_{11}^{ab} therefore agree in ev-

TABLE I. Three distinct abelianizations. The first is the abelianized Artin action of Ref. [14]; the second carries the exponent sum of Ref. [11]; the third carries the full intertwining matrix, Eq. (4).

Map	Target	Survives
Artin action on $H_1(D_n)$	permutations	the permutation
$B_n \to B_n^{\mathrm{ab}}$	$\mathbb{Z}$	exponent sum
$P_n \to P_n^{\mathrm{ab}}$	$\mathbb{Z}^{n(n-1)/2}$	the RRR matrix

[1] The period at which the abelian data first collide depends on the labeling one fixes. Numbering the points in visiting order, as here, the first collision we find is at period 11. Taking instead the conjugacy-invariant image in P_n^{ab}, the natural object for Eq. (3), the orbits $s9^{13}$ and $s9^{15}$ of Ref. [11] already agree: their matrices coincide after $i \mapsto 4i \bmod 9$, which carries the successor cycle to another generator of the same cyclic group, while their entropies are 0.604904 and 0.491993.

ery entry. The six fall into at least two braid types, with topological entropies 0.538349 and 0.512786, heights 2/7 and 1/4, and depths 1/2 and 2/5 [19]; we recomputed the entropies from the orbit codes with train tracks [20]. The identification is realized among tabulated orbits: whatever separates the two types lies in $[P_{11}, P_{11}]$. Outside such a restricted family the collapse can be total, as the example below shows. The saddle–node selection rule of Ref. [1] is an abelian statement: it constrains merging orbits through their rotation rates alone.

Three neighboring constructions should be kept distinct from Eq. (4). Hall defines the linking number of one orbit about another as a homology class in the suspension manifold, and his Lemma 1.6 exhibits orbits of equal braid type with different linking numbers about a third orbit [15]. There is no conflict with Eq. (4), which compares braids of one fixed collection of strands, while the lemma varies the collection. The framed-braid linking matrix of Ref. [21] classifies a template, not an orbit braid. And Boyland's abelian Nielsen equivalence [13] is the same quotient performed on the abelianized fundamental group of the surface rather than on the group of braids.

The Nielsen–Thurston theorem sorts braids into three classes: periodic (finite order), reducible, and pseudo-Anosov [9, 12]. Periodic braids, some power of which is a power of the full twist, have zero topological entropy, and on them the abelian data are complete. A theorem of Birman, Gebhardt, and González-Meneses states that once two braids are known to be periodic, their conjugacy is decided in *linear* time by comparing exponent sums [22]. The coarsest abelian invariant is a complete conjugacy invariant exactly on the periodic class. Zero entropy alone does not suffice: a reducible braid whose pieces are periodic also has zero entropy without being periodic. The torus knots in the horseshoe catalog show this at work. They are finite-order orbits, and their self-rotation-rate spectra identify them on sight [9, Sect. 4.5].

Two topological models appear in this literature: the pseudo-Anosov representative of a braid, and a template [23]. The pseudo-Anosov representative is a minimal model: every map carrying the braid has at least its topological entropy [24] and at least its periodic orbits [13], and the physical system may have more. A template carries a subshift of finite type [25], a full shift for the horseshoe, so it bounds the entropy and the orbit set from above. It typically has too many orbits, which must be *pruned* to arrive at a tighter bound [26, 27].

Abelian data can also indicate chaos, and the mechanism deserves a precise statement. The rotation number of an orbit about a fixed point is its linking number divided by its period [15]. For torus homeomorphisms isotopic to the identity, a rotation set with nonempty interior forces positive topological entropy [28]. For disc maps the analogous interval alone forces nothing: an integrable twist realizes a whole rotation interval about its fixed point at zero entropy. Entropy certification on the disc or annulus needs a twist or embedding hypothesis

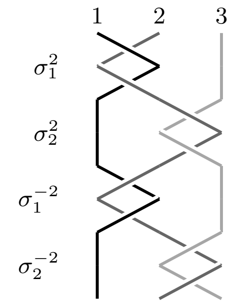

FIG. 1. The pure braid $\beta = \sigma_1^2\sigma_2^2\sigma_1^{-2}\sigma_2^{-2} = [A_{12}, A_{23}]$ on three strands, read downward. Strands 1 and 2 cross four times, twice with each sign; strands 2 and 3 likewise; strands 1 and 3 never cross. Every linking number vanishes, so every relative rotation rate of a three-orbit collection braided as β is zero, while β is pseudo-Anosov with dilatation $(2+\sqrt{5})^2$ and topological entropy 2.887 per period.

beyond the abelian data [13, Sect. 8]. Within a cataloged family the abelian data can identify a chaotic invariant set directly. The exponent sum measured from a bouncing-ball time series did so "without the calculation of more detailed quantities such as fractal dimensions or Lyapunov exponents" [11]. What the abelian data cannot do is determine the braid type, or the value of a dilatation or an entropy.

As an example consider the group P_3 which can be realized physically by three stirring rods in a mixing tank [14]. Take the generators $A_{12} = \sigma_1^2$ and $A_{23} = \sigma_2^2$ and form their commutator (Fig. 1),

$$\beta = [\sigma_1^2, \sigma_2^2] = \sigma_1^2\sigma_2^2\sigma_1^{-2}\sigma_2^{-2} \in [P_3, P_3]. \tag{5}$$

Strands 1 and 2 cross four times, twice with each sign; strands 2 and 3 likewise; strands 1 and 3 never cross. All three linking numbers vanish, so a collection braided as β has every relative rotation rate equal to zero, in the self-entries and the mutual entries alike. The braid is nonetheless pseudo-Anosov. The Burau representation is faithful for $n \leq 3$ [14, 18]. Specialized to $t = -1$ it maps B_3 onto $\mathrm{SL}(2, \mathbb{Z})$ with only a central kernel, and a 3-braid is pseudo-Anosov exactly when its image is hyperbolic, the dilatation being the leading eigenvalue [14]. The image of β is $\left(\begin{smallmatrix}13 & 8\\ 8 & 5\end{smallmatrix}\right)$, with trace 18, so β is pseudo-Anosov with dilatation $\lambda = 9 + 4\sqrt{5} = (2+\sqrt{5})^2$ and entropy $h(\beta) = 2\ln(2+\sqrt{5}) = 2.887\,271$ per period. Every homeomorphism carrying this braid has at least this entropy. The entropy of a surface homeomorphism is bounded below by the growth rate of its action on the fundamental group [29, 30]. For a disc map that growth rate is bounded below by the spectral radius of the Burau matrix at any $|t| = 1$ [31, 32]. Three orbits with every rotation rate zero force topological entropy of at least 2.887. For a stirring device, this is a protocol indistinguishable by rotation rates from one that mixes poorly. Powers of β, or longer commutators, push the bound as high as desired, so vanishing abelian data are compatible with arbitrarily large entropy.

The rotation rates were adopted when the non-abelian data were out of reach. Train-track methods "are impractical for periods much greater than 10" [19], and the braid-conjugacy algorithms available in 1994 were judged "probably not an effective solution for braids beyond period 8" [11]. Boyland stated the general terms of the trade: a stronger orbit equivalence "encodes more information about the orbit, but as usual, recording more information results in diminished computability" [13]. Under those constraints an abelian proxy, measurable directly from data, was a good choice. Algorithmic advances have since opened new possibilities. The Nielsen–Thurston type of a braid can be decided in quadratic time at fixed strand number [33]. The dilatation and invariant foliations of a pseudo-Anosov class are computed in quadratic time, again at fixed strand number [34]. Conjugacy itself, the computational core of braid-type equality, is polynomial for periodic braids [22] and lies in NP$\cap$co-NP at fixed strand number [35]. Dynnikov coordinates yield closed-form dilatation polynomials for infinite braid families at every braid index [36]. Free software implements all of this: Hall's `trains` and `Dynn` [20], Thiffeault and Budišić's `braidlab` [37], and Bell's `flipper` [38]. Of these, `braidlab` builds the braid directly from trajectory data, the same input from which rotation rates have always been measured [14, 37].

We recommend computing both kinds of invariant. The intertwining matrix remains the right first computation: it is cheap, it is measurable, it fixes the template, it is complete on the finite-order orbits, and within a cataloged family it can signal chaos. When the question is what the orbits force—type, dilatation, entropy, forcing order—the braid itself is now no harder to compute. Equation (4) says the extra information is not stored anywhere in the rotation rates.

In summary, we have shown that the relative rotation rates of a collection of periodic orbits are the abelianization of its pure braid. They are complete conjugacy data precisely on the periodic braids. The non-abelian remainder is now computationally tractable and can join the rotation rates in fingerprinting chaotic invariant sets. Braid invariants are not restricted to dissipative systems: with a choice of section and suspension, they extend to two-degree-of-freedom autonomous Hamiltonian systems such as the restricted three-body problem. Periodic solutions have organized celestial mechanics since Poincaré [39]. Braids can be used in a variety of ways to provide an even finer dissection of invariant structures in both dissipative and conservative nonlinear dynamical systems, such as occur in celestial mechanics [40, 41].

ACKNOWLEDGMENTS

We thank R. Gilmore, H. G. Solari and G. B. Mindlin for their patient explanations on characterizing chaotic systems. We thank T. Hall and J.-L. Thiffeault, whose tables, algorithms, and software make the closing recommendation a practical one.

DATA AVAILABILITY

No new data were generated. The orbit codes and tabulated invariants used here are those of Table III of Ref. [11]; the topological entropies quoted were recomputed from those codes with the `trains` package [20].

[1] H. G. Solari and R. Gilmore, "Relative rotation rates for driven dynamical systems," Phys. Rev. A **37**, 3096 (1988).

[2] N. B. Tufillaro, H. G. Solari, and R. Gilmore, "Relative rotation rates: Fingerprints for strange attractors," Phys. Rev. A **41**, 5717 (1990).

[3] G. B. Mindlin, X.-J. Hou, H. G. Solari, R. Gilmore, and N. B. Tufillaro, "Classification of strange attractors by integers," Phys. Rev. Lett. **64**, 2350 (1990).

[4] R. Gilmore, "Topological analysis of chaotic dynamical systems," Rev. Mod. Phys. **70**, 1455 (1998).

[5] G. B. Mindlin, H. G. Solari, M. A. Natiello, R. Gilmore, and X.-J. Hou, "Topological analysis of chaotic time series data from the Belousov–Zhabotinskii reaction," J. Nonlinear Sci. **1**, 147 (1991).

[6] N. B. Tufillaro, R. Holzner, L. Flepp, E. Brun, M. Finardi, and R. Badii, "Template analysis for a chaotic NMR laser," Phys. Rev. A **44**, R4786 (1991).

[7] F. Papoff, A. Fioretti, E. Arimondo, G. B. Mindlin, H. G. Solari, and R. Gilmore, "Structure of chaos in the laser with saturable absorber," Phys. Rev. Lett. **68**, 1128 (1992).

[8] N. B. Tufillaro, P. Wyckoff, R. Brown, T. Schreiber, and T. Molteno, "Topological time-series analysis of a string experiment and its synchronized model," Phys. Rev. E **51**, 164 (1995).

[9] R. Gilmore and M. Lefranc, *The Topology of Chaos: Alice in Stretch and Squeezeland*, 2nd ed. (Wiley-VCH, Weinheim, 2011).

[10] R. Gilmore, "How topology came to chaos," in *Topology and Dynamics of Chaos: In Celebration of Robert Gilmore's 70th Birthday*, edited by C. Letellier and R. Gilmore (World Scientific, Singapore, 2013), p. 169.

[11] N. B. Tufillaro, "Braid analysis of a bouncing ball," Phys. Rev. E **50**, 4509 (1994).

[12] W. P. Thurston, "On the geometry and dynamics of diffeomorphisms of surfaces," Bull. Am. Math. Soc. **19**, 417 (1988).

[13] P. Boyland, "Topological methods in surface dynamics," Topology Appl. **58**, 223 (1994).

[14] J.-L. Thiffeault, *Braids and Dynamics*, Frontiers in Applied Dynamical Systems: Reviews and Tutorials, Vol. 9 (Springer, Cham, 2022).

[15] T. Hall, "The creation of horseshoes," Nonlinearity **7**, 861 (1994).

[16] N. B. Tufillaro, T. Abbott, and J. Reilly, *An Experimental Approach to Nonlinear Dynamics and Chaos* (Addison-Wesley, Reading, MA, 1992).

[17] A. de Carvalho and T. Hall, "Conjugacies between horseshoe braids," Nonlinearity **16**, 1329 (2003).

[18] J. S. Birman, *Braids, Links, and Mapping Class Groups*, Annals of Mathematics Studies, Vol. 82 (Princeton University Press, Princeton, NJ, 1974).

[19] T. Hall, "Weak universality in two-dimensional transitions to chaos," Phys. Rev. Lett. **71**, 58 (1993).

[20] T. Hall, `trains` and `Dynn`, software available at `https://www.liverpool.ac.uk/~tobyhall/T_Hall.html`.

[21] P. Melvin and N. B. Tufillaro, "Templates and framed braids," Phys. Rev. A **44**, R3419 (1991).

[22] J. S. Birman, V. Gebhardt, and J. González-Meneses, "Conjugacy in Garside groups III: Periodic braids," J. Algebra **316**, 746 (2007).

[23] R. W. Ghrist, P. J. Holmes, and M. C. Sullivan, *Knots and Links in Three-Dimensional Flows*, Lecture Notes in Mathematics Vol. 1654 (Springer-Verlag, Berlin, 1997).

[24] B. Farb and D. Margalit, *A Primer on Mapping Class Groups*, Princeton Mathematical Series Vol. 49 (Princeton University Press, Princeton, NJ, 2011).

[25] D. Lind and B. Marcus, *An Introduction to Symbolic Dynamics and Coding* (Cambridge University Press, Cambridge, 1995).

[26] A. de Carvalho and T. Hall, "How to prune a horseshoe," Nonlinearity **15**, R19 (2002).

[27] P. Cvitanović, G. H. Gunaratne, and I. Procaccia, "Topological and metric properties of Hénon-type strange attractors," Phys. Rev. A **38**, 1503 (1988).

[28] J. Llibre and R. S. MacKay, "Rotation vectors and entropy for homeomorphisms of the torus isotopic to the identity," Ergodic Theory Dyn. Syst. **11**, 115 (1991).

[29] R. Bowen, "Entropy and the fundamental group," in *The Structure of Attractors*, Lecture Notes in Mathematics, Vol. 668 (Springer, Berlin, 1978), pp. 21–29.

[30] A. Manning, "Topological entropy and the first homology group," in *Dynamical Systems—Warwick 1974*, Lecture Notes in Mathematics, Vol. 468 (Springer, Berlin, 1975), pp. 185–190.

[31] B. Kolev, "Entropie topologique et représentation de Burau," C. R. Acad. Sci. Paris Sér. I **309**, 835 (1989).

[32] D. Fried, "Entropy and twisted cohomology," Topology **25**, 455 (1986).

[33] M. Calvez, "Fast Nielsen–Thurston classification of braids," Algebr. Geom. Topol. **14**, 1745 (2014).

[34] D. Margalit, B. Strenner, S. J. Taylor, and S. Ö. Yurttaş, "Quadratic-time computations for pseudo-Anosov mapping classes," arXiv:2408.07596.

[35] M. C. Bell, "The pseudo-Anosov and conjugacy problems are in NP $\cap$ co-NP," arXiv:1410.1358.

[36] T. Hall and S. Ö. Yurttaş, "On the topological entropy of families of braids," Topology Appl. **156**, 1554 (2009).

[37] J.-L. Thiffeault and M. Budišić, "`braidlab`: A software package for braids and loops," arXiv:1410.0849; `https://github.com/jeanluct/braidlab`.

[38] M. C. Bell, `flipper`, software available at `https://github.com/MarkCBell/flipper`.

[39] H. Poincaré, *Les Méthodes nouvelles de la mécanique céleste* (Gauthier-Villars, Paris, 1892–1899); English translation: *New Methods of Celestial Mechanics*, edited by D. L. Goroff (American Institute of Physics, New York, 1993).

[40] C. Moore, "Braids in classical dynamics," Phys. Rev. Lett. **70**, 3675 (1993).

[41] R. Montgomery, "The N-body problem, the braid group, and action-minimizing periodic solutions," Nonlinearity **11**, 363 (1998).